Supplementary Material (ESI) for *PCCP*

Hydrolysis of Cisplatin - A Metadynamics Study
Supporting Information

Justin Kai-Chi Lau[a] *and Bernd Ensing**[b]
Department of Chemistry and Applied Bioscience, ETH Zurich, USI Campus,
Computational Science, Via Giuseppe Buffi 13, CH-6900, Lugano, Switzerland

[a] Current address: Department of Chemistry, Hong Kong Baptist University, Kowloon Tong , Hong Kong, Email: justin@hkbu.edu.hk
[b] Current address: Van't Hoff Institute for Molecular Sciences, University of Amsterdam, Nieuwe Achtergracht 166, 1018 WV Amsterdam, Netherlands, Email: ensing@science.uva.nl

Table S1: Bond lengths (Å) comparisons between the CPMD and Gaussian results.

cutoff	70	80	90	100	Gaussian98
			cisplatin		
Pt-N	2.118	2.121	2.119	2.120	2.119
Pt-Cl	2.317	2.316	2.316	2.316	2.350
			cis-$[Pt(NH_3)_2(OH_2)Cl]^+$		
Pt-N[a]	2.049	2.050	2.049	2.049	2.051
Pt-N[b]	2.138	2.139	2.138	2.139	2.136
Pt-Cl	2.291	2.289	2.290	2.290	2.325
Pt-O	2.126	2.128	2.124	2.126	2.129
			cis-$[Pt(NH_3)_2(OH_2)_2]^{2+}$		
Pt-N	2.052	2.052	2.053	2.053	2.055
Pt-O	2.125	2.121	2.121	2.125	2.128

[a] NH_3 in the position trans to H_2O
[b] NH_3 in the position trans to Cl

Table S2: Comparison on the reaction ΔE_r and activation ΔE_a energies predicted by CPMD and Gaussian in gas phase

cutoff	70	80	90	100	110	120	B3LYP	MP2	CCSD(T)
				first hydrolysis					
ΔE_r	117.5	117.5	117.6	117.6	117.7	117.7	117.8	119.3	116.9
ΔE_a	18.4	18.6	18.7	18.7	18.8	18.8	18.9	19.4	17.9
				second hydrolysis					
ΔE_r	215.1	215.0	215.0	215.1	215.1	215.2	214.1	214.7	213.7
ΔE_a	20.2	20.4	20.6	20.7	20.7	20.7	20.9	21.6	21.0

Table S3: Properties of liquid water compared. Peak maxima R_{Ow-Hw} and R_{Ow-Ow} are given in Å. The coordination numbers CN_{Ow-Hw} and CN_{Ow-Ow} were estimated by integration of the first peak of g_{Ow-Hw} and g_{Ow-Ow} up to the next minimum.

	R_{Ow-Hw}	CN_{Ow-Hw}	R_{Ow-Ow}	CN_{Ow-Ow}
Simulation A	1.90	1.9	2.75	4.0
Simulation B	1.90	1.9	2.76	3.8
Simulation C	1.91	1.8	2.76	3.7
CPMD[a]			2.75-2.85	4.0-5.0
neutr. diff[b]	1.9	1.6-1.9	2.86	5.3
X-ray[c]	-	-	2.7-2.8	4.3

[a] Ref. 1 other CPMD work using different functionals
[b] Ref. 2 using neutron diffraction
[c] Ref. 3, 4 using X-ray diffraction

Table S4: Properties of ligands of Pt complexes and free Cl− (Cl') in water. Peak maxima are given in Å. The coordination numbers CN were estimated by integration of the first peak up to the next minimum.

	cis-$[Pt(NH_3)_2Cl_2]$		cis-$[Pt(NH_3)_2(OH_2)Cl]^+$		cis-$[Pt(NH_3)_2(OH_2)_2]^{2+}$	
ligand	r^{peak}	CN	r^{peak}	CN	r^{peak}	CN
N-O_w	2.95	2.9	2.95	3.5	2.96	4.0
Cl-H_w	2.25	1.7	2.26	2.4	-	-
Cl-O_w	(3.23)*	(2.9)*	3.15	3.4	-	-
O-O_w	-	-	2.77	1.0	2.66	2.0
Cl'-H_w	-	-	2.23	4.0	2.16	4.0
Cl'-O_w	-	-	3.17	4.3	3.15	4.5

*The rdf $g_{Cl\text{-}Ow}$ does not show a first peak. See text.

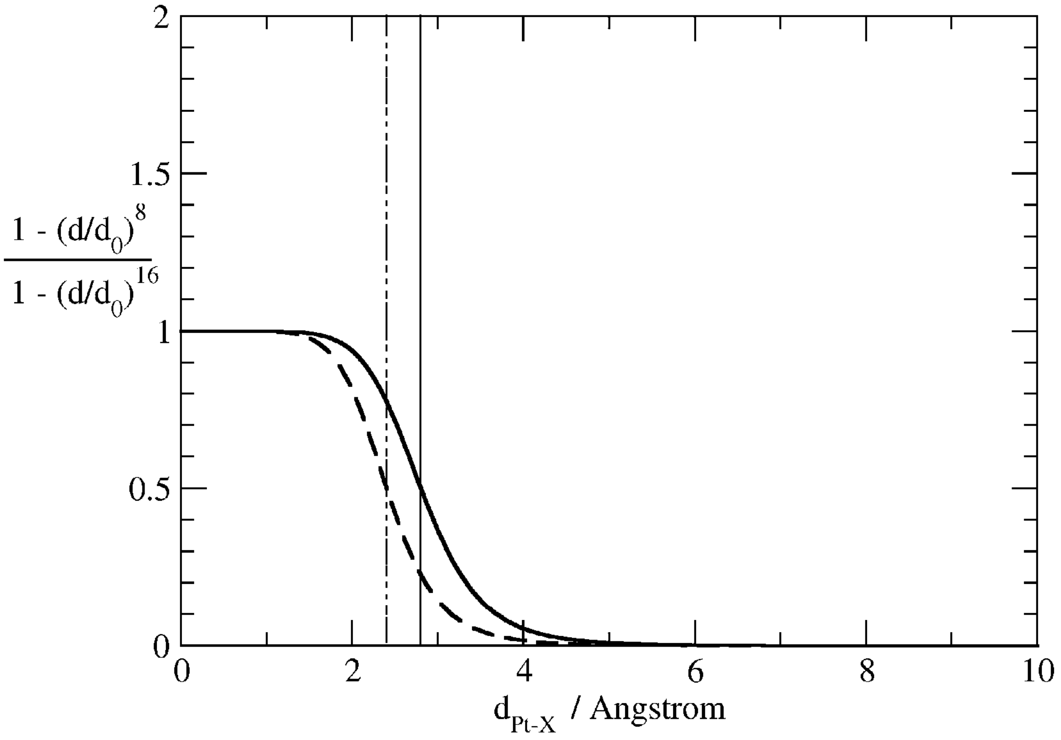

Figure S1: Graph of the switchfunctions used in the coordination number collective variable defined in equation 1 (also in the text). Solid line: switchfunction centered at $d_0 = 2.8$ Å; dashed line: switchfunction centered at $d_0 = 2.4$ Å. For example in the case for $CN_{Pt\text{-}O}$, the number of water molecules within the first coordination shell of the Platinum is estimated, using a cut-off distance d_0=2.4 Å, by summing over all N_X=50 water molecule oxygen atoms. Most water molecules are of course much farther away from Pt than d_0 and will contribute a number close to zero to the sum. Only water molecules closer than d_0 contribute a number close to 1, resulting in practise a good estimate of the actual coordination number. Note that the function is also differentiable at $d=d_0$, as is easily shown using l'Hôpital's rule. For details of using coordination numbers as reaction coordinates, see Ref. 5.

$$CN_{Pt-X} = \sum_{i}^{N_X} \frac{1-\left(\frac{d_{Pt-X}}{d_0}\right)^8}{1-\left(\frac{d_{Pt-X}}{d_0}\right)^{16}} \qquad (1)$$

Figure S2: Fluctuations of Platinum-ligand atom distances in cis-[Pt$(NH_3)_2Cl_2$] (top-row graphs obtained from simulation A), cis-[Pt$(NH_3)_2(OH_2)Cl]^+$ (middle-row graphs obtained from simulation B), and cis-[Pt$(NH_3)_2(OH_2)_2]^{2+}$ (bottom-row graphs obtained from simulation C).

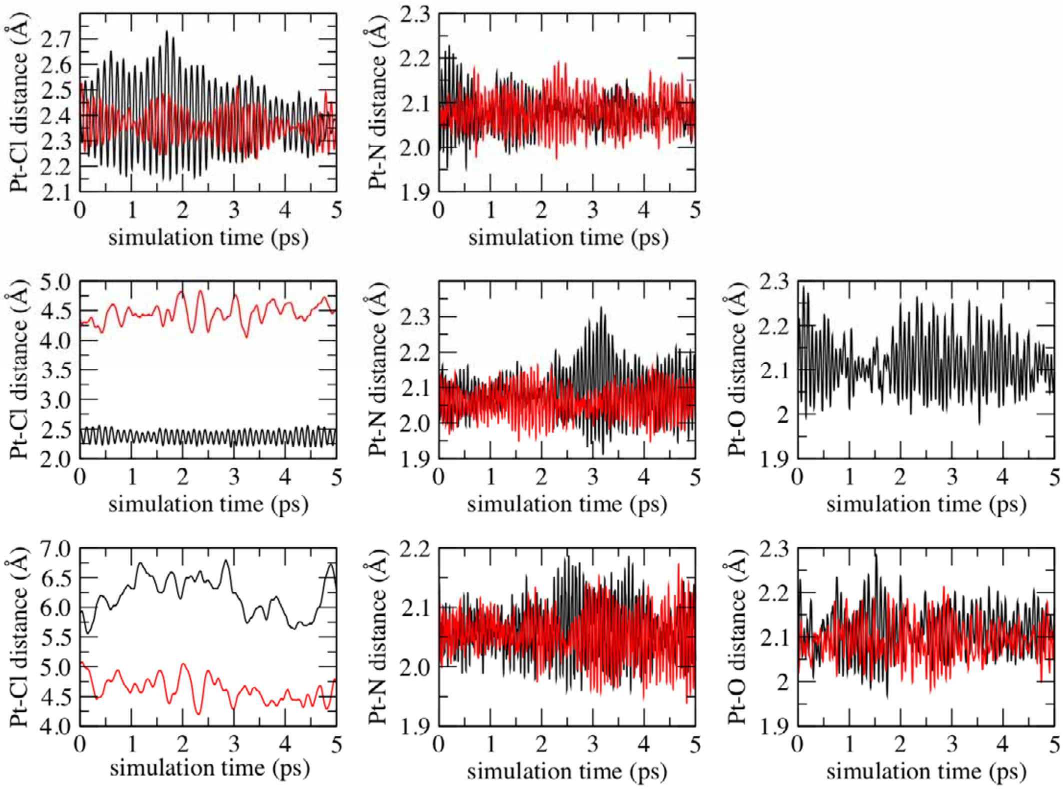

Figure S3: Radial distribution of solvent water around the Platinum ion in cis-$[Pt(NH_3)_2Cl_2]$ (left panel from simulation A), cis-$[Pt(NH_3)_2(OH_2)Cl]^+$ (middle panel from simulation B), and cis-$[Pt(NH_3)_2(OH_2)_2]^{2+}$ (right panel from simulation C). Although the curves show noise due to the relatively short (5 ps) CPMD trajectories, we can clearly observe an increase in solvent structure in the Pt-O distributions (solid lines) going from the neutral cisplatin (left) to the doubly hydrolyzed cis-$[Pt(NH_3)_2(OH_2)_2]^{2+}$ complex (right). Note also that the Pt-H distribution (dashed lines) shows some amplitude at short distances (2-3 Angstrom) attributed to occasional hydrogen bonding at the axial platinum positions (see also figure S4), which subsequently disappears upon hydrolysis.

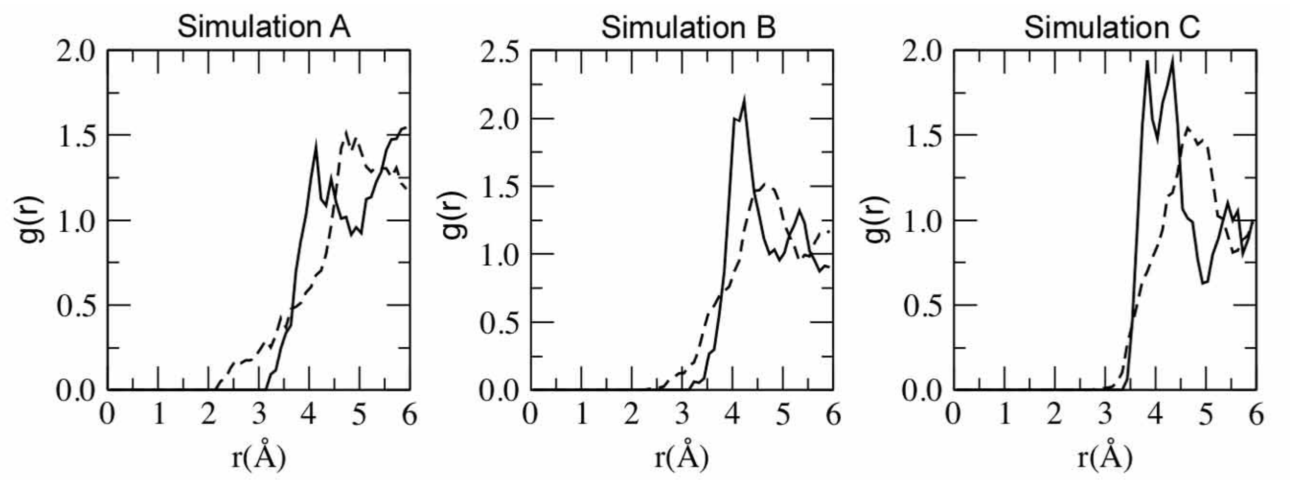

Figure S4: Representative snapshots of the aqueous cis-[$Pt(NH_3)_2Cl_2$] (left panel, from simulation A), cis-[$Pt(NH_3)_2(OH_2)Cl]^+$ (middle panel from simulation B), and cis-[$Pt(NH_3)_2(OH_2)_2]^{2+}$ (right panel, from simulation C). The cisplatin complex is seen to interact through weak H-bonding with water at the axial position, indicated by the dashed line in the left panel. Note the square planar structure for all three complexes and the position of the Cl^- anion forming a contact ion pair through hydrogen bonding with a water ligand in simulations B and C.

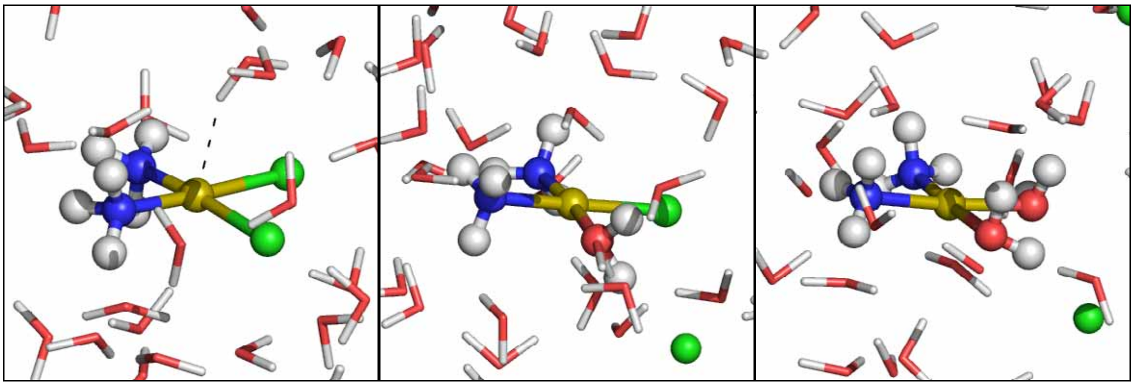

Color coding of the complex shown in ball-and-stick representation:

Pt yellow; Cl green; N blue; O red; H white.

Solvent water molecules are represented by red and white sticks

Figure S5: Fluctuations of coordination numbers during the forward (upper) and backward (lower) reactions.

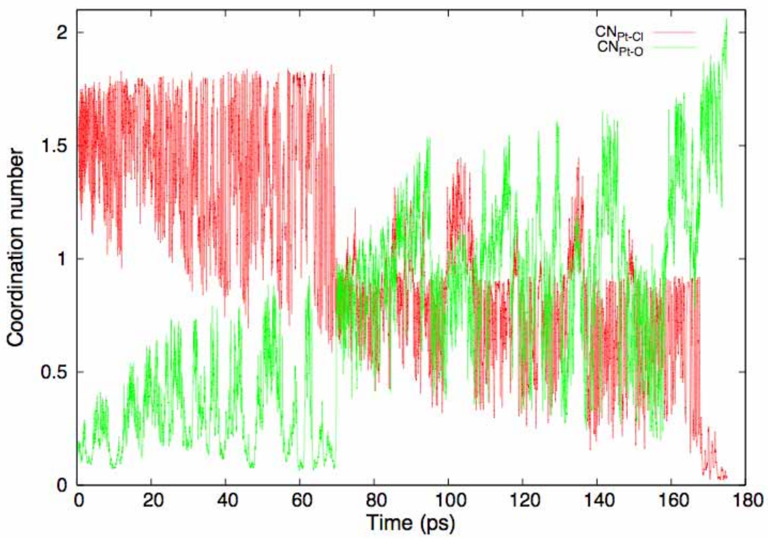

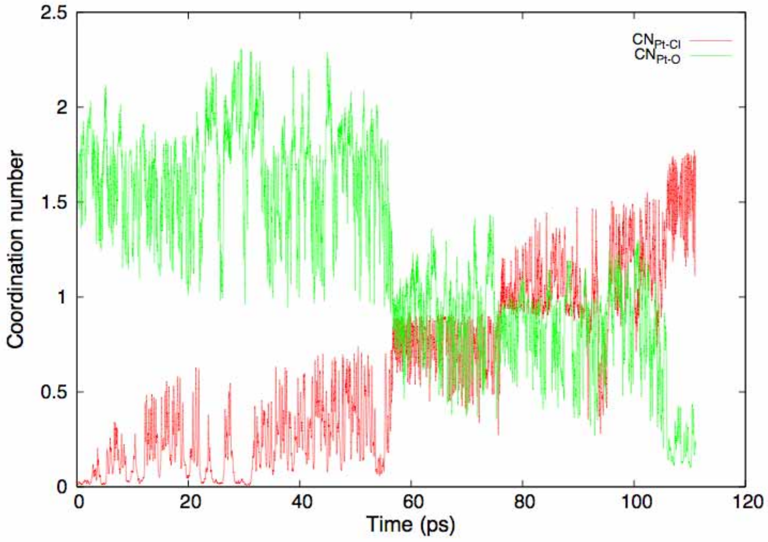

Figure S6: Histogram showing the overlapped windows in the umbrella samplings. Upper graph: Simulation F; Middle graph: Simulation G; Lower graph: Simulation H

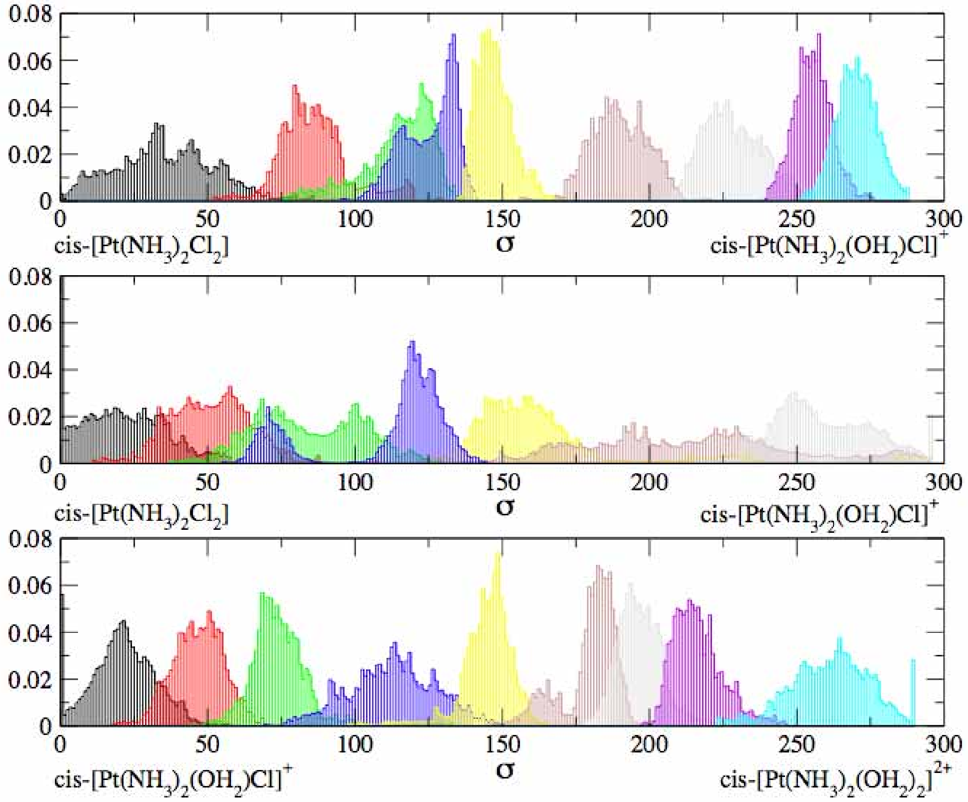

Figure S7: Free energy profile for the first hydrolysis of cisplatin along the lowest free energy path from metadynamics (green), after smoothing the metadynamics curve for umbrella sampling (red), and final result after umbrella sampling. On the x-axis, σ characterizes the reaction coordinate defined as the parameterized curve that follows the lowest free energy path as determined with the nudge elastic band method, using 300 points (arbitrary units).

The green curve was obtained from the metadynamics simulation starting from the reactant state (cis-[$Pt(NH_3)_2Cl_2$] minimum at the left side, which then crossed the transition state and started filling the intermediate cis-[$Pt(NH_3)_2(OH_2)Cl]^+$ minimum at the right side with Gaussian bias potentials. However, this minimum was not filled up to the initial transition state because the system escaped via the second transition state to the final $[Pt(NH_3)_2(OH_2)_2]^{2+}$ state, giving rise to a too high metadynamics result on the right. Although this was largely repaired in the subsequent umbrella sampling simulations (black curve), we only use the barrier height of 23.3 kcal/mol and obtain the barrier for the reverse process from the backward metadynamics simulation shown in Figure S8.

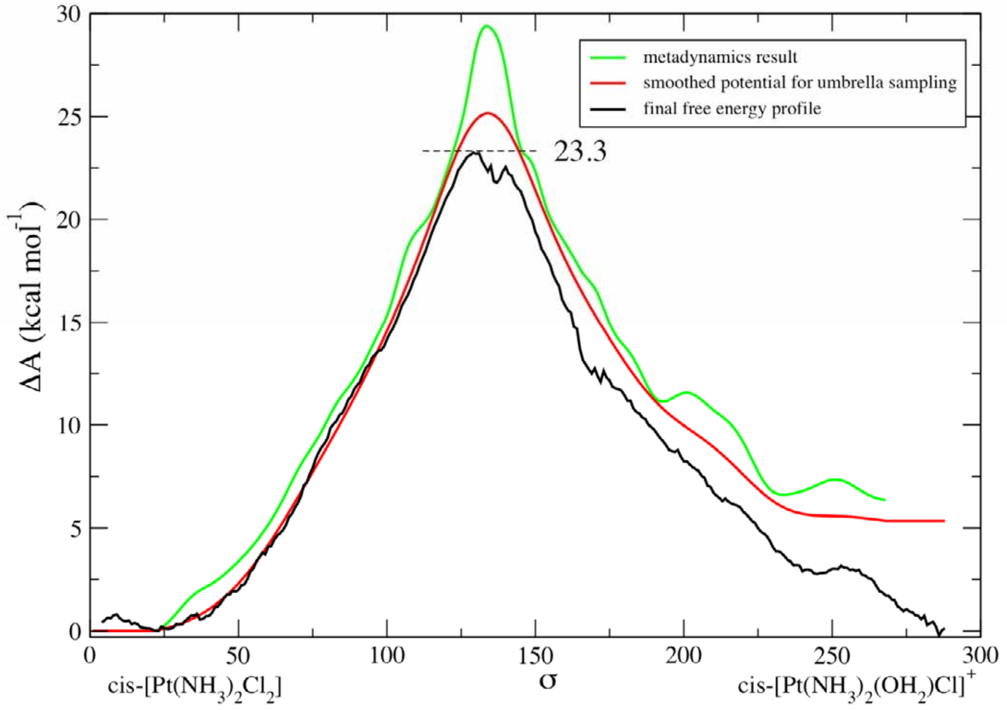

Figure S8: Free energy profile (reverse barrier) for the first hydrolysis of cisplatin along the lowest free energy path from metadynamics (green), after smoothing the metadynamics curve for umbrella sampling (red), and final result after umbrella sampling. On the x-axis, σ characterizes the reaction coordinate defined as the parameterized curve that follows the lowest free energy path as determined with the nudge elastic band method, using 300 points (arbitrary units).

The green curve was obtained from the metadynamics simulation of the hydrolysis reactions in the reverse direction starting from the intermediate cis-$[Pt(NH_3)_2(OH_2)Cl]^+$ minimum at the right side, which then crossed the transition state and "dropped" into the cis-$[Pt(NH_3)_2(Cl_2)]$ minimum at the left side, after which the metadynamics simulation was stopped. This final state was thus not filled with Gaussians again, so that the metadynamics result is too high on the left side. This is partly remedied by the subsequent umbrella sampling simulations (black line). However, contrary to the forward reaction shown in Figure S7 in which case we allowed the simulation to sample the intermediate until the system escaped over the second transition state, here instead the final (left-hand-side) minimum was poorly sampled (see also the contour plot in Figure 5) so that the location of this minimum and the pathway from the transition state to this minimum can be expected to have somewhat larger uncertainties. We therefore only take the free energy barrier for the reverse process and obtain the forward barrier from the metadynamics/umbrella sampling simulations of the forward process shown in Figure S7.

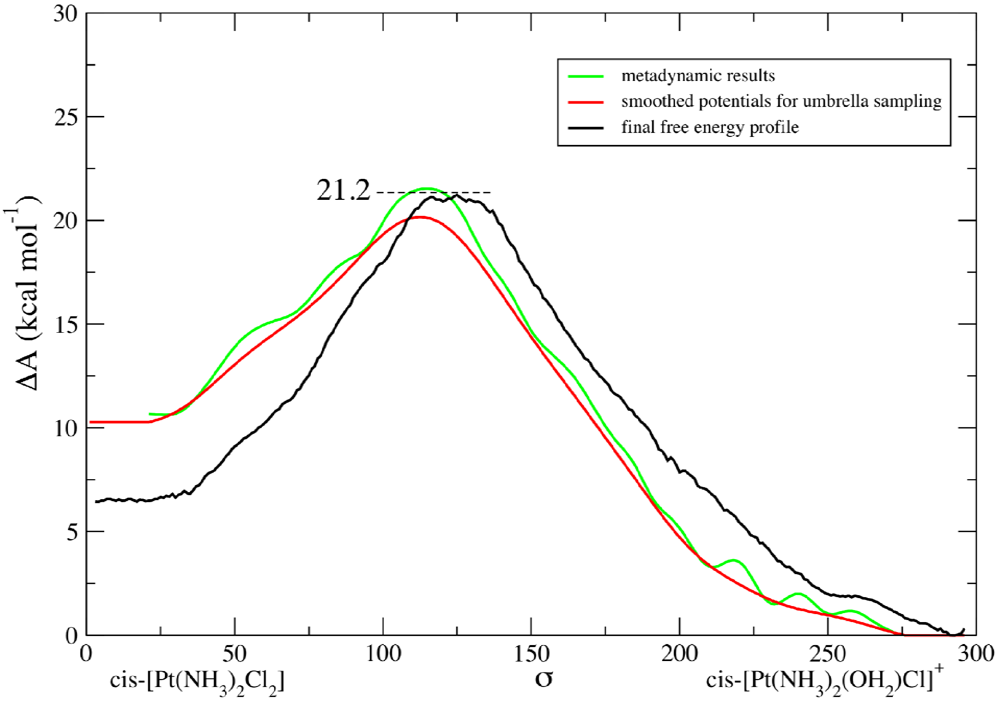

Figure S9: Free energy profile for the (reverse) second hydrolysis of cisplatin along the lowest free energy path from metadynamics (green), after smoothing the metadynamics curve for umbrella sampling (red), and final result after umbrella sampling. On the x-axis, σ characterizes the reaction coordinate defined as the parameterized curve that follows the lowest free energy path as determined with the nudge elastic band method, using 300 points (arbitrary units).

For this second hydrolysis reaction, we found very similar positions for the stable states as well as similar pathways for the forward and the backward metadynamics simulations. Here the metadynamics result (green line) obtained for the second hydrolysis reaction in the reverse direction (that is, starting in the right-hand-side minimum and moving to the left) shows how both minima were effectively sampled and filled with Gaussian hills (in contrast to the metadynamics simulations for the first hydrolysis reaction, see Figures S7 and S8), resulting in a rather good estimate of the free energy landscape as shown by the final umbrella sampling result (black line).

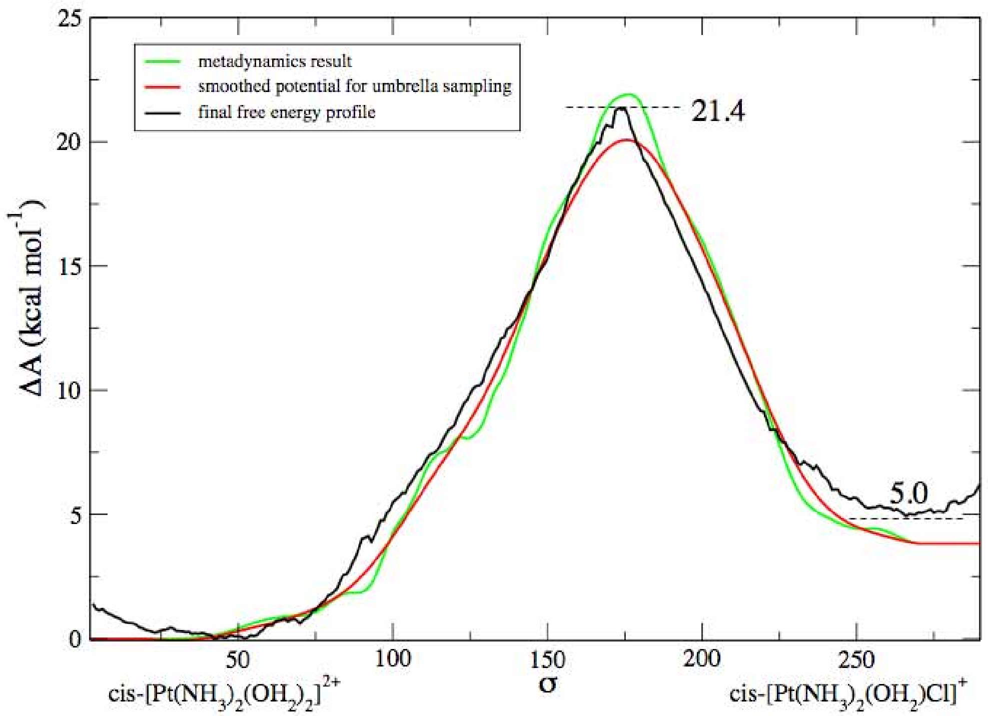

References

1. Sprik, M.; Hutter, J.; Parrinello, M. *J. Chem. Phys.*, **1996**, *105*, 1142.
2. Tromp, R. H.; Posterino, P.; Neilson, G. W.; Ricci, M. A.; Soper, A. K. *J. Chem. Phys.*, **1994**, *101*, 6210.
3. Narten, A. H.; Danford, M. D.; Levy, H. A. *Discussions Faraday Soc.*, **1967**, *43*, 97.
4. Narten, A. H.; Levy, H. A. *J. Chem. Phys.*, **1971**, *55*, 2263.
5. Sprik, M. *Faraday Discuss.*, **1998**, *110*, 437.